Behavioral/Cognitive

Behavioral Oscillations in Attention: Rhythmic α Pulses Mediated through θ Band

Kun Song,[1,3]* Ming Meng,[2] Lin Chen,[1] Ke Zhou,[1] and Huan Luo[1]*

[1]State Key Laboratory of Brain and Cognitive Science, Institute of Biophysics, Chinese Academy of Sciences, Beijing, 100101, China, [2]Department of Psychological Brain Sciences, Dartmouth College, Hanover, New Hampshire 03755, and [3]University of Chinese Academy of Sciences, Beijing, 100049, China

Neuronal oscillations are ubiquitous in the brain and contribute to perception and attention. However, most associated evidence derives from *post hoc* correlations between brain dynamics and behavior. Although a few recent studies demonstrate rhythms in behavior, it remains largely unknown whether behavioral performances manifest spectrotemporal dynamics in a neurophysiologically relevant manner (e.g., the temporal modulation of ongoing oscillations, the cross-frequency coupling). To investigate the issue, we examined fine spectrotemporal dynamics of behavioral time courses in a large sample of human participants ($n = 49$), by taking a high time-resolved psychophysical measurement in a precuing attentional task. We observed compelling dynamic oscillatory patterns directly in behavior. First, typical attentional effects are demonstrated in low-pass (0–2 Hz) filtered time courses of behavioral responses. Second, an uninformative peripheral cue elicits recurring α-band (8–20 Hz) pulses in behavioral performances, and the elicited α pulses for cued and uncued conditions are in a temporally alternating relationship. Finally, ongoing α-band power is phase locked to ongoing θ-bands (3–5 Hz) in behavioral time courses. Our findings constitute manifestation of oscillations at physiologically relevant rhythms and power-phase locking, as widely observed in neurophysiological recordings, in behavior. The findings suggest that behavioral performance actually consists of rich dynamic information and may reflect underlying neuronal oscillatory substrates. Our data also speak to a neural mechanism for item attention based on successive cycles (θ) of a sequential attentional sampling (α) process.

Key words: **α pulse; behavioral rhythm; cross-frequency coupling; precuing; rhythmic sampling; θ phase**

Introduction

Neuronal oscillations are ubiquitous in brain signals at disparate spatial scales and have been proposed to be closely associated with various cognitive functions (Buzsaki, 2006). For example, converging evidence from neurophysiological recordings demonstrate that neuronal γ-band (30–70 Hz) rhythms subserve attention and perception processes, by means of binding-by-synchronization or communication-by-coherence (Desimone and Duncan, 1995; Singer and Gray, 1995; Siegel et al., 2008). Moreover, numerous electroencephalography (EEG) studies and neurophysiological recordings reveal prominent α-band (8–13 Hz) rhythms and disclose its suppressive nature in selective visual attention (Worden et al., 2000; Ward, 2003; Thut et al., 2006; Händel et al., 2007; Klimesch et al., 2007; Palva and Palva, 2007; Bollimunta et al., 2008, 2011; Mo et al., 2011; Rohenkohl and Nobre, 2011). In addition, θ-band (3–8 Hz) rhythms have been suggested to mediate perception, memory, and attention (e.g., Lisman and Idiart, 1995; Landau and Fries, 2012; Luo et al., 2013). Importantly, oscillatory phase mediates perception (Busch and VanRullen, 2010), sensory stream processing (Luo and Poeppel, 2007, 2012; Luo et al., 2010; Kayser et al., 2012; Ng et al., 2012), attention (Schroeder and Lakatos, 2009), and memory formation (Luo et al., 2013) by modulating cortical excitability in a cyclic manner (Thut et al., 2012) and segmenting inputs into appropriate chunks in time (Giraud and Poeppel, 2012).

On the other hand, because of the inherent temporal limitations of conventional psychophysical methods, most behavioral studies assess attentional processes at a much coarser temporal scale and therefore cannot access possible rapid fluctuations in behavioral performance. Indeed, most associated evidence supporting the central role of brain oscillations is built upon *post hoc* relationships between recorded brain oscillations and behavioral performances. Recently, a few studies have demonstrated rhythms in psychophysical measurements (Fiebelkorn et al., 2011; VanRullen and Dubois, 2011; Landau and Fries, 2012; de Graaf et al., 2013) and suggested that the underlying neuronal oscillations may have direct consequences on behavior. However, it still remains largely unknown whether behavioral performances manifest spectrotemporal dynamics in a neurophysiologically relevant manner

Received Nov. 18, 2013; revised Feb. 19, 2014; accepted Feb. 24, 2014.

Author contributions: K.Z. and H.L. designed research; K.S. and H.L. performed research; K.S., M.M., L.C., K.Z., and H.L. contributed unpublished reagents/analytic tools; K.S. and H.L. analyzed data; M.M., K.Z., and H.L. wrote the paper.

This work was supported by the Ministry of Science and Technology of China Grant 2012CB825500, National Nature Science Foundation of China Grants 31171075, 91120019, 31171081, and 91132302, and Chinese Academy of Sciences Strategic Priority Research Program B Grants XDB02010100 and XDB02050001. We thank Jessica Goold for improving the English style; Chengyang Tao, Prof. Jianfeng Feng, and Dr. Dan Zhang for statistics and data analysis consultancy; Ruihuai Zhang for part of data collection; Chencan Qian for helping with eyetracker recording; and Fan Wang and Kun Hu for technical support.

The authors declare no competing financial interests.

*K.S. and H.L. contributed equally to this work.

Correspondence should be addressed to either Dr. Huan Luo or Dr. Ke Zhou, State Key Laboratory of Brain and Cognitive Science, Institute of Biophysics, Chinese Academy of Sciences, 15 Datun Road, Beijing, 100101, China. E-mail: luohuan@gmail.com or kzhou.bcslab@gmail.com.

DOI:10.1523/JNEUROSCI.4856-13.2014

 0270-6474/14/344837-08$15.00/0

(e.g., the temporal modulation of ongoing oscillations, the cross-frequency coupling). Motivated by a psychophysical method probing behavioral performance using a high time-resolved measurement (e.g., Landau and Fries, 2012), we directly examined the fine-grained time course, particularly the spectrotemporal profile, and the rhythmic characteristics of behavioral performance in covert attention.

Specifically, we used a precuing paradigm (Posner and Cohen, 1984; Klein, 2000) to examine the temporal course of covert spatial attention. As illustrated in Figure 1*A*, subjects were asked to covertly attend to two peripheral boxes. An uninformative (cue validity: 50%) peripheral cue appeared near to one of the two boxes. After a varying interval (cue-to-target stimulus-onset asynchrony [SOA]: 0.2–1.1 s) from the onset of the cue, a target occurred in one of the two peripheral boxes. Subjects were requested to discriminate the target shape as fast as possible and the reaction time (RT) was recorded. The cue and the target occurred either in the same (valid) or opposite locations (invalid). Critically, to investigate the fine temporal structure of spatial attention, we used a time-resolved measure by ranging the cue-to-target SOA from 0.2 s to 1.1 s in steps of 0.02 s (see Fig. 1*A*), corresponding to a 50 Hz sampling frequency.

Materials and Methods

The study was approved by the ethics committee of the Institute of Biophysics at Chinese Academy of Sciences, Beijing. Fifty subjects (24 females, all right handed, average age 23 years) participated in peripheral cuing. All subjects had normal or corrected-to-normal visual acuity and provided informed consent. They were paid as compensation for their time. One subject was excluded from further analysis because of poor shape discrimination performance.

Behavioral tasks. Subjects sat in a dark room 84.5 cm in front of a CRT monitor (100 Hz), and their heads were stabilized in a chin rest. Their responses were recorded through a parallel port response keypad. In each trial, subjects were requested to maintain fixation at a central cross (0.46° × 0.46°) and covertly attend to two peripheral boxes (2.46° × 2.46°) presented 5.45° on either side of the fixation cross. After 1.3–1.8 s, a cue was briefly presented for 0.1 s; and 0.2–1.1 s after the cue onset (cue-to-target SOA), a target (a white square or a circle, 1.85° × 1.85°) was presented for 0.15 s, within either the left (LVF) or the right (RVF) peripheral boxes. Subjects were asked to report the shape of the target as fast as possible while maintaining high discrimination accuracy. The peripheral boxes and fixation cross were medium gray (14.1 cd/m^2); the background was gray (4.3 cd/m^2); the cue and target were white (30.4 cd/m^2). A peripheral bar cue was presented 7.7° on either side of the fixation cross, and the target randomly and with equal likelihood appeared on either the same side (valid) as the cue or the opposite side (invalid), corresponding to an uninformative 50% cue validity. Subjects were informed of the cue validity before the experiment. Eye movements were monitored using an eyetracker (SMI RED120, 120 Hz) on a subset of subjects and results showed that they maintained good fixation on the central cross (within 1°) throughout the experimental trials (data not shown). Notably, to achieve a dense temporal assessment of behavioral performance, we used a time-resolved measure, such that the target could appear at one of 46 temporal intervals, in steps of 20 ms, from 0.2 s to 1.1 s after cue onset, corresponding to a sampling frequency of 50 Hz. To achieve a more prominent effect of cue resetting, the number of trials for SOA of 200 ms was 10 times of that for other SOAs (Fiebelkorn et al., 2011). Each subject completed 880 trials in total, in four separate blocks interleaved with 5 min breaks. The SOA of each trial was pseudorandom from 0.2 s to 1.1 s, balanced across trials to have exactly the same likelihood (except more trials at 0.2 s, the shortest cue-to-target SOA, for reasons specified above).

Data analyses. Behavioral RT data were analyzed with MATLAB (MathWorks) partly using functions from the EEGLAB toolbox (Delorme and Makeig, 2004), wavelet toolbox, and CircStat toolbox (Berens, 2009). For each subject, RTs that were >4 SDs across all trials were excluded from further analysis. The remaining RTs were then normalized within each subject separately, to remove the large variance between individuals in overall motor responses. Specifically, in each subject, RTs in all trials under all conditions (different SOAs, valid and invalid conditions, etc.) were regarded as the RT distribution for that subject. The *z*-score for each trial's RT was then computed by demeaning and then dividing by the SD of the RT distribution. It is worth noting that, after the within-subject normalization, the relative relationship among RTs of all trials in each subject was kept intact, although the RT values were normalized ~0. For each of the four conditions (valid vs invalid for target at LVF, valid vs invalid for target at RVF), the temporal profile of the normalized RTs was calculated as a function of cue-to-target SOA from 0.2 to 1.1 s, in steps of 0.02 s (50 Hz sampling frequency).

Our main goal was to examine the fine spectrotemporal dynamics of behavioral time courses. To do so, we analyzed the RT temporal courses within different frequency bands (Filtering analysis), the time-frequency contents of RT profiles (Time-frequency analysis), the phase relationship between different conditions (Phase lag analysis), and the cross-frequency modulation (Power-phase locking analysis). Finally, to remove the classical effects of attention and expectancy, we detrended RT profiles (Analysis of detrended RT time courses).

Filtering analysis. To investigate the RT profiles within different frequency bands, the RT temporal profile for each condition (valid vs invalid for LVF, valid vs invalid for RVF) was zero-padded (50 points before and after the RT temporal profile), multiplexed by a Hanning window, and then filtered (two-pass least-squares FIR filtering, 10th order, EEGLAB toolbox) within different cutoff frequency bands (0–2, 2–5, and 8–20 Hz), in each subject separately.

Time-frequency analysis. To assess the RT profiles as a function of time (cue-to-target SOA) and frequency, the RT temporal profile for each condition was transformed using the continuous complex Gaussian wavelet (order = 4; e.g., FWHM = 1.32 s for 1 Hz wavelet) transforms (Wavelet toolbox, MATLAB), with frequencies ranging from 1 to 25 Hz in steps of 2 Hz. The power profile of RTs (squared absolute value) as a function of time and frequency was then extracted from the output of the wavelet transform. Differences in power profile between valid and invalid conditions were calculated. This time-frequency analysis was performed for each condition and for each subject separately. The grand mean of time-frequency power was then averaged across subjects.

We further performed a randomization procedure to assess the statistical significance of the difference between the power profiles for valid and invalid conditions, by shuffling the RT time series across valid and invalid conditions within each subject. After each randomization, the same time-frequency analysis was performed on the surrogate signals, as that performed in the original RT data analysis, and the time-frequency power difference profile between valid and invalid conditions was recalculated. This procedure was repeated 200 times and resulted in a distribution of valid–invalid power difference at each time-frequency point, from which the $p < 0.05$ threshold (uncorrected) was obtained. Two methods of multiple-comparison correction were then further applied to the uncorrected randomization threshold time-frequency map: within-frequency correction and cross-frequency correction. For within-frequency correction, the maximum or the minimum values across all time bins within each frequency were set as the threshold for the frequency. For cross-frequency correction, the maximum or the minimum across all time and frequency bins were set as the threshold.

Phase lag analysis. To examine the θ phase relationship between valid and invalid conditions within the time range (cue-to-target SOA: 0.4–1.1 s), as observed in 2–5 Hz bandpass filtered RTs (see Fig. 3*A*, middle), we extracted the unfiltered temporal profile of RTs within this time range (0.4–1.1 s), which were zero-padded, Hanning tapered, and then 128-point Fourier transformed. The phase difference within 2–5 Hz between valid and invalid conditions was calculated and averaged (CircStats toolbox) for each subject separately. Nonuniformity for valid–invalid phase differences across subjects was then tested using circular statistics (Rayleigh test for nonuniformity for circular data in CircStats toolbox).

Power-phase locking analysis. The RT temporal profiles were zero-padded (50 points before and after the RT temporal profile) and multiplexed by a Hanning window in each condition and each subject

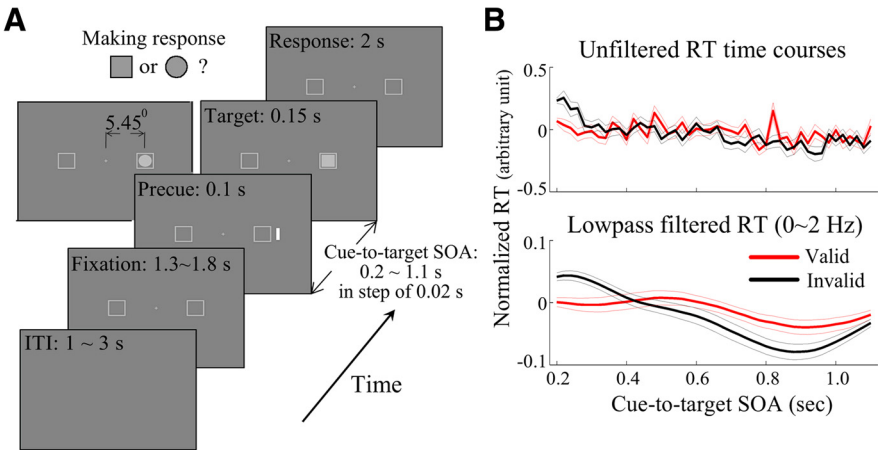

Figure 1. Experiment paradigm and replication of typical behavioral results in 0–2 Hz RT time courses. ***A***, Subjects fixated a central cross and covertly attended to two peripheral boxes. After a varying interval (cue-to-target SOA: 0.2~1.1 s) from the onset of the cue (an uninformative bar near one of the two peripheral boxes), a target (a circle or a square) occurred within either the cued box (valid) or the uncued box (invalid). Subjects were requested to determine the target shape, and the RT was recorded. To achieve a more prominent effect of cue resetting, the number of trials for SOA of 0.2 s was 10 times of that for other SOAs. ***B***, RT time courses (normalized within-subject across all trials) as a function of cue-to-target SOA ($N = 49$). Grand average unfiltered RT time courses (top, mean ± SEM) and 0–2 Hz low-pass filtered RT time courses (bottom, mean ± SEM), for valid (red) and invalid (black) conditions.

separately. The power time series was then calculated by bandpass filtering (two-pass least-squares FIR filtering, 10th order, EEGLAB toolbox) the zero-padded RT time courses ± 2 Hz of frequencies from 4 to 19 Hz in steps of 1 Hz and extracting the power time course from the Hilbert transform of the bandpass filtered signals. The phase time series was calculated by band-passing filtering (two-pass least-squares FIR filtering, 10th order, EEGLAB toolbox) the same zero-padded RT time courses ± 1 Hz of frequencies from 2 to 16 Hz in steps of 1 Hz but extracting the phase time course from the Hilbert transform of the bandpass filtered signals. Furthermore, to avoid possible power edge effects after bandpass filtering (weak power around onset and offset of time series), the temporal epochs from 0.3 to 1 s (instead of original 0.2–1.1 s) in power time series and phase time series were used for further power-phase locking analysis.

To assess the strength of the power-phase locking, for each power frequency (4–19 Hz in steps of 1 Hz) and phase frequency (2–16 Hz in steps of 1 Hz), a vector of power-phase time series (power as the length, θ phase as the angle) was constructed, from which the mean resultant vector throughout all time points and all conditions was calculated for each subject. The length of the mean vector was defined as the strength of the power-phase locking for this specific power frequency and phase frequency. To test the statistical significance of locking strength, the time series of power was shuffled and the strength of power-phase locking was recalculated 200 times, resulting in a permutation distribution for each power frequency and phase frequency, based on which the $p < 0.05$ threshold map (as a function of phase frequency and power frequency) was determined. Further multiple-comparison corrections were performed by setting the maximum values across the whole threshold map as the power-phase locking threshold, which was then compared with the original power-phase locking map.

To specifically assess the relationship between θ-band (2–5 Hz) phase and the power at other frequencies, the θ-band phase time series was calculated by 2–5 Hz bandpass filtering (two-pass least-squares FIR filtering, 10th order, EEGLAB toolbox) the zero-padded RT time courses (50 points before and after the RT temporal profile, then multiplexed by a Hanning window) and extracting the phase time course from the Hilbert transform of the bandpass filtered signals. The phase values were then binned into 8 ranges from $-\pi$ to $+\pi$. The corresponding power at other frequencies (2–20 Hz) in each of the value ranges of the θ phase was then averaged, resulting in a power-phase locking matrix as a function of θ phase ($-\pi$ to $+\pi$) and frequency (2–20 Hz) for each subject. This analysis was performed for each condition and each subject separately.

Analysis of detrended RT time courses. In each subject, a simple model representing the classical attentional effect time course as well as the expectation trend was first constructed, by calculating the 300 ms (in steps of 20 ms) moving average of the RT time courses for each condition (valid and invalid). These trend signals were then subtracted from the corresponding RT time courses to obtain the detrended RT time courses for each condition. The same time-frequency analysis as described earlier was then performed on the detrended RT time courses. Furthermore, spectrum analysis was performed on the RT time courses before and after detrending for comparison.

Results

Low-frequency RT time courses demonstrate patterns that resemble the classical effects of attention

Subjects performed well in the task (percentage correct: 0.98 ± 0.0014), and only a small number of trials were discarded because of either no response or out-of-range RTs (trial discarding percentage: 0.007 ± 0.0004). Figure 1*B* illustrates the raw normalized RT time courses (normalized across all trials within each subject separately) as a function of cue-to-target SOAs (top) under valid (red) and invalid (black) conditions. Interestingly, although the raw normalized RT time courses were noisy and fluctuated largely, our results matched well with classical findings (Posner and Cohen, 1984; Klein, 2000) when the RT time courses were 0–2 Hz low-pass filtered (Fig. 1*B*, bottom). Specifically, early enhancements (SOA < 0.4 s) and subsequent sustained reductions ("inhibition of return," Klein, 2000) were found for the valid condition (cue and target occurred at the same location) compared with the invalid condition (cue and target occurred at the opposite location). The demonstration of typical attentional effects in the low-pass filtered RTs is not the result of filter ringing effects, and we obtained the same results from 10-point moving averaged RT time courses. These results thus confirmed that our approach, despite using a much higher time-resolved measure than previous studies, was reliable and effective in reproducing effects of attention. It is noteworthy that those typical attention effects were manifested only in the low-frequency range here, consistent with previous studies that had probed behavioral performance at SOAs every several hundred milliseconds, equivalent to an assessment of low-pass filtered psychophysical data. Moreover, although having more trials for the shortest SOA here (Fig. 1*A*; see Materials and Methods), we observed similar attentional time course patterns as in classical findings of attentional effects, suggesting little influences of the present design on the classical attentional behavior.

Rhythmic α pulses in RT time courses

Next, we performed a spectrotemporal analysis on RT time courses to examine their fine dynamic structures after cue onset, as a function of frequency (0–25 Hz) and time (cue-to-target SOA: 0.2–1.1 s). Surprisingly, α band (~8–20 Hz) showed interesting power response profiles. Specifically, as shown in Figure 2*A*, the valid condition manifested stronger α power in RT time courses than the invalid condition, in a pulsed manner (at ~0.5 s and ~0.8 s), for both LVF and RVF in which the target was presented, but more prominent for the LVF (Fig. 2*A*, top). More-

over, the initiated intermittent α-pulse profiles by valid and invalid cues were in a type of out-of-phase relationship (switching between negative and positive values in Fig. 2*A*). As illustrated in Figure 2*B*, the switching relationship in elicited α pulses between the valid and invalid conditions could be clearly seen for the LVF (left) but were much weaker for the RVF (right). Therefore, after attention on one of the two peripheral locations was reset by a cue, RT time courses in cued and uncued locations underwent pulsed α-rhythm fluctuations, modulated at approximately a θ rhythm (3–5 Hz, every ~300 ms), in an alternating manner. The findings thus disclose rich spectrotemporal dynamics in behavioral performance and suggest a close link between α-band activity and attention processes, consistent with previous electrophysiological studies (Ward, 2003; Thut et al., 2006; Klimesch et al., 2007; Bollimunta et al., 2008, 2011; Händel et al., 2011; Mo et al., 2011; Rohenkohl and Nobre, 2011; Romei et al., 2012).

To test whether the classical effects of attention (early facilitation and late inhibition) or the effects of expectancy (decreased RT as SOA increases) could explain the observed time-frequency profiles (i.e., the alternating α pulses), we further conducted analysis with detrended RT time courses (Fig. 3*A*). The spectrotemporal dynamics were reexamined after removing the classical attentional and expectancy effects, which mainly occurred in low frequencies instead of in α-band (spectrum analysis, Fig. 3*C*). As illustrated in Figure 3*B*, the detrended RT time courses (Fig. 3*A*, bottom) showed similar spectrotemporal profiles, suggesting that our findings in the α-band could not be explained by the classical effects of attention and expectancy.

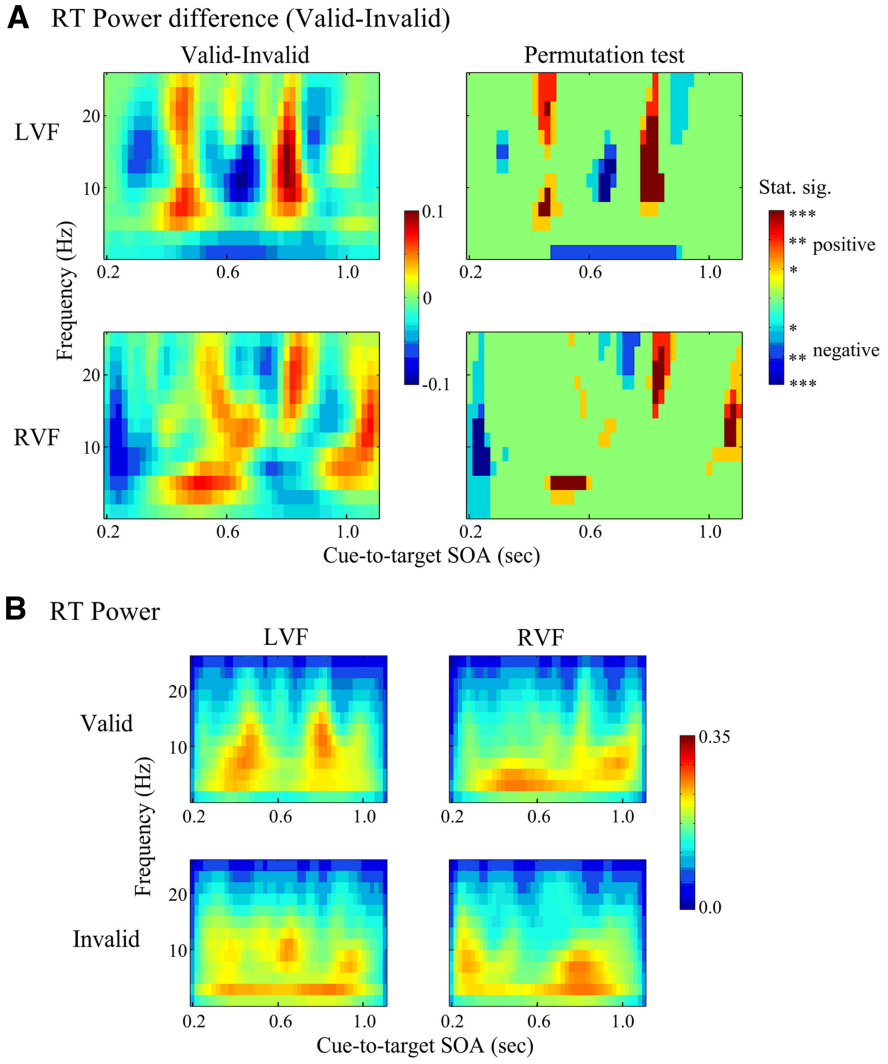

Figure 2. Time-frequency power profile for RT time courses as a function of cue-to-target SOA (0.2–1.1 s) and frequency (0–25 Hz). ***A***, Left, Grand average time-frequency plots ($n = 49$) for valid–invalid power difference when target was presented on LVF (upper) or RVF (lower). Right, Valid–invalid power difference time-frequency plots thresholded by permutation test. *Uncorrected $p < 0.05$ (within-frequency multiple-comparison correction). **$p < 0.05$ (within-frequency multiple-comparison correction). ***$p < 0.05$ (across-frequency multiple-comparison correction). Red represents positive valid–invalid power difference values; blue represents negative difference. ***B***, Grand average time-frequency power ($n = 49$) for valid (top) and invalid condition (bottom), when target was presented on LVF (left) or RVF (right).

Cued-uncued phase lag in θ-band

Based on the findings that α pulses initiated in valid and invalid conditions were modulated at a θ rhythm (3–5 Hz) and were in a type of switching relationship, one might predict that RT time courses in the θ range, although showing no effects in power (Fig. 2*A*), demonstrate certain valid–invalid phase relationships. This θ-band phase hypothesis also derives from a recent study that revealed phase lagged 4 Hz fluctuations in detection performance (Landau and Fries, 2012). We therefore further investigated the θ range, by bandpass (2–5 Hz) filtering the RT time courses. As shown in Figure 4*A* (middle), after early facilitation (SOA < 0.4 s), the θ-band filtered RTs for the invalid condition started to lag behind that of the valid condition consistently at LVF, a signature of a valid–invalid phase relationship. Further phase analysis on the unfiltered RTs during this temporal range (Fig. 4*A*, middle, square) demonstrated that the valid–invalid phase lag within θ range (2–5 Hz) was not uniformly distributed across subjects (Fig. 4*B*; Rayleigh test, $N = 49$, $p = 0.049$) and clustered around a mean of −100°. Such a phase relationship was observed neither in RVF (Rayleigh test, $N = 49$, $p = 0.46$) nor in α band (Rayleigh test, $N = 49$, $p = 0.39$). Thus, in the LVF, in addition to intermittent α-band pulses, cuing initiated 4 Hz RT fluctuations that had a consistent phase lag between cued and uncued locations.

α power is locked to ongoing θ phase in RT time courses

Figure 4*A* summarized the RT profiles within different frequency bands. First, 0–2 Hz filtered RTs demonstrated typical peripheral cuing results consisting of early facilitation and late inhibition (top). Second and most critically, the spectrotemporal analysis revealed prominent roles of θ phase (middle) and α power (bottom) in exogenous attention modulation, reflected in behavioral measurements. Notably, α power seemed to be modulated by a θ rhythm (Fig. 2). Therefore, it is natural to ask whether the ongoing α power was locked to θ phase in the present behavioral data of fine-scale temporal resolution, as widely revealed in electro-

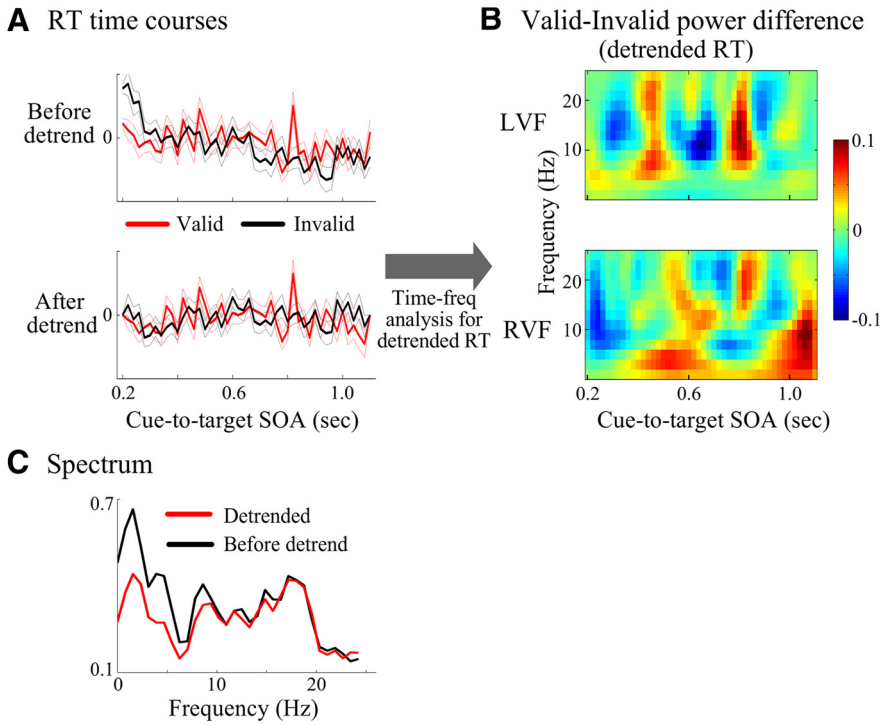

Figure 3. Time-frequency power profile and spectrum for detrended RT time courses. ***A***, Grand average RT time course ($n = 49$) as a function of cue-to-target SOA before (upper) and after detrending (lower). The detrended RT time course (bottom) showed a rather flat fluctuating pattern lacking classical attentional and expectancy effects. ***B***, Grand average time-frequency plots ($n = 49$) for valid–invalid power difference for the detrended RT time courses, when target was presented in LVF (upper) or RVF (lower). The detrended RTs showed a similar valid–invalid power difference profile as in Figure 2*A*. ***C***, Grand average spectrum ($n = 49$) for RT time courses before (black) and after detrending (red). After detrending, the RT time courses manifested decreased power mainly in low frequencies.

physiological data (Canolty et al., 2006). To avoid possible power edge effects that may affect the power-phase locking result, we extracted power and phase values of the middle part of RT time courses (0.3–1.0 s; Fig. 4*A*, bottom, square) for further power-phase locking analysis. As illustrated in Figure 4*C* (middle), α power was indeed locked to θ phase, such that stronger α power occurred at the θ phase centered ~0°. We further calculated the cross-frequency power-phase locking in a wide range of frequencies, and only the θ band was found to be phase locked to α power (Fig. 4*C*, left, dotted box; permutation test with multiple-comparison corrected, $p < 0.05$). Moreover, the α-θ power-phase coupling was a rather general phenomenon. It was found for both valid and invalid conditions in both LVF and RVF (Fig. 4*C*, right). The results thus implicate that the α pulses, taking turns to occur at cued and uncued locations, might be indeed phase modulated by the θ rhythms, through a phase-amplitude coupling manner.

Discussion

We examined the fine spectrotemporal dynamics of covert attention in a classical precuing paradigm, by probing behavioral performance at 50 Hz. Typical peripheral precuing effects (Posner and Cohen, 1984; Klein, 2000), including early facilitation and late inhibition, were observed in 0–2 Hz RT time courses. Most importantly, we demonstrated that an uninformative peripheral cue initiated recurring α (8–20 Hz) pulses in RT time courses alternatively at cued and uncued locations, at a θ (2–5 Hz) rhythm. Furthermore, ongoing α power was phase locked to θ band (2–5 Hz), consistent with previous results of neurophysiological recordings (Canolty et al., 2006), suggesting a θ-mediating α-sampling process in exogenous attention. Our findings present evidence for the manifestation of oscillations at multiple physiologically relevant rhythms in behavior (e.g., α, θ), implicating a neural mechanism for multi-item attention based on successive cycles (θ) of a sequential attentional sampling (α) process.

It is well established that brain oscillations are associated with sensory processing, perception, and attention (Desimone and Duncan, 1995; Singer and Gray, 1995; Ward, 2003; Buzsaki, 2006; Klimesch et al., 2007; Siegel et al., 2008; Fries, 2009; Schroeder and Lakatos, 2009; Giraud and Poeppel, 2012; Jensen et al., 2012; Thut et al., 2012). Accumulating evidence, including our own (Luo and Poeppel, 2007, 2012; Luo et al., 2010, 2013), suggests that brain oscillatory dynamics act as an internal temporal context, based on which neural ensembles are dynamically formed and dissolved to mediate sensory processing, perception, memory, consciousness, and attention (Lisman and Idiart, 1995; Klimesch, 1999; Buschman and Miller, 2009; Doesburg et al., 2009; Schroeder and Lakatos, 2009; Thut et al., 2011, 2012; Buschman et al., 2012; Giraud and Poeppel, 2012; Jensen et al., 2012; Kayser et al., 2012). However, unlike neurophysiological and EEG/MEG studies, most behavioral studies only examine attentional processes at a much coarser temporal scale and therefore cannot access possible rapid fluctuations in behavioral performance. The manifestation of oscillations in behavioral performance is somewhat only recent in its origin (VanRullen et al., 2007; Fiebelkorn et al., 2011; VanRullen and Dubois, 2011; Landau and Fries, 2012; de Graaf et al., 2013). For example, a recent study showed that, after resetting attention to one of two spatial locations, visual detection performance at these two locations underwent a 4 Hz fluctuation in an antiphase manner (Landau and Fries, 2012). Here, we also observed a phase lag relationship in θ band, thus consistent with previous studies in supporting the central role of θ oscillations in mediating rhythmic attention sampling. However, instead of RVF dominance in the out-of-phase effect found in a previous study, we mainly observed the effect in LVF, which might be due to several aspects. For example, LVF and RVF were sorted in the previous study based on the location of cue, whereas we followed previous precuing behavioral paradigms (Posner and Cohen, 1984; Klein, 2000) to compare valid and invalid conditions according to the side on which the target was presented. Meanwhile, it is noteworthy that, although the alternating α pulses occurred only in LVF in the present study, we observed a similar but much weaker trend in RVF. Therefore, further studies need to be performed to systematically compare the oscillatory performances between LVF and RVF.

Moreover and more critically, there are two distinct and novel aspects of the present findings. First, previous studies observed fluctuations mainly in low-frequency bands (e.g., δ, θ, low-α) and examined the rhythm in a more stationary way (e.g., presence of specific frequency or estimating parameters from computa-

tional modeling) or used rhythmic sensory stimulation to drive α-band rhythms in visual behavior. Here, we directly examined the dynamic profile of attentional behavioral performance (e.g., the temporal modulation of ongoing oscillations, the cross-frequency coupling) and demonstrated α-band pulses mediated by a θ rhythm in RT time courses. This provides new evidence suggesting that the widely observed α rhythms in human EEG recordings may have direct functional consequences in behavior and play a causal role in spatial attention. Second, the present study is the first, to our knowledge, to reveal the power-phase nesting relationship between high-frequency and θ rhythms in behavioral performances, although this relationship has been widely observed in neurophysiological and EEG/MEG recordings (e.g., Canolty et al., 2006). The findings thus further support a cross-frequency dynamic framework underlying attentional behavior. Our results may take us one step further beyond the traditional correlational approach to assess the role of brain oscillations in behavior, by directly assessing the spectrotemporal dynamics of behavioral results.

Furthermore, a key aspect of our observations concerns the α-band pulses in behavioral performances modulated by attention. Notably, posterior α activity is the strongest spontaneous signal widely observed in human EEG recordings and has been linked to functional inhibition during attention, such that the unattended visual stream is associated with strong α power (Worden et al., 2000; Thut et al., 2006; Klimesch et al., 2007; Händel et al., 2011; Rohenkohl and Nobre, 2011). Recent thanslaminar animal recordings, investigating the physiological mechanisms generating α, have demonstrated cortical origins of α-band activities and their close association with attentional modulation (Bollimunta et al., 2008, 2011; Mo et al., 2011). Moreover, α activity has been suggested to exercise a phasic force on neuronal excitability by generating pulses of inhibition (Ward, 2003). The phase of the α-band EEG activities that occurred before stimulus onset modulates the detection of the subsequent stimulus (Busch and VanRullen, 2010; Thut et al., 2011; Romei et al., 2012). During task rule changes, α-band activity in monkey prefrontal cortex was enhanced on task-irrelevant neuronal ensembles before increased high-frequency synchrony on task-relevant populations (Buschman et al., 2012), indicating the inhibition function of α-band rhythms in rule selection. Recently, it has also been proposed that the periodic inhibitory nature of α oscillation may provide a mechanism for prioritizing unattended stimuli based on salience (Jensen et al., 2012). In our study, the invalid condition showed stronger α pulses than the valid condition at short SOAs when attention was actually captured to the cued locations, thus providing further support to the inhibitory nature of α rhythm. Therefore, our results are in line with the critical role of α rhythm in attention inhibition and its pulsed manner.

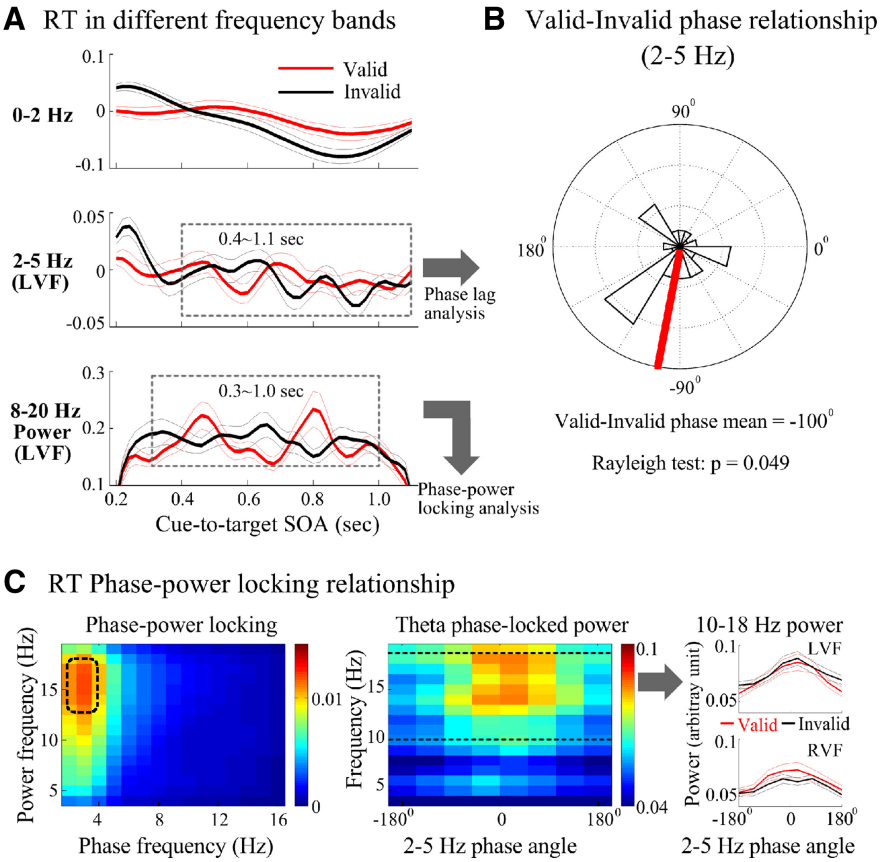

Figure 4. θ-band phase lag and α-θ power-phase coupling in RT time courses. ***A***, Top, The 0–2 Hz filtered RT time courses as a function of cue-to-target SOA for valid (red) and invalid (black) conditions. Middle, θ-band (2–5 Hz) filtered RT time courses in LVF, with dotted box indicating the time range (0.4–1.1 s) for further phase lag analysis. Bottom, Power response for α-band (8–20 Hz) filtered RT time courses in LVF, with dotted box indicating the time range (0.3–1.0 s) for further phase-power locking analysis. ***B***, Polar plots for the distribution ($n = 49$) of θ-band (2–5 Hz) phase lag between valid and invalid conditions in the RT time courses in LVF during the time range (***A***, middle, dotted box, 0.4–1.1 s). Red line indicates the mean valid–invalid θ phase difference. ***C***, Phase-power locking in RT time course during the time range (***A***, bottom, dotted box, 0.3–1.0 s). Left, Grand mean cross-frequency phase-power locking ($n = 49$). Middle, Grand mean power response ($n = 49$) as a function of frequency (4–20 Hz) and θ-band phase (−180° to 180°). Dotted line indicates the upper and lower boundary for α-band range (8–20 Hz). Right, Grand mean ($n = 49$, mean ± SEM) α-band power (8–20 Hz, range between two dotted lines in left panel) as a function of θ-band (2–5 Hz) phase (−180° to 180°) for valid (red) and invalid (black) conditions, when target was presented in LVF (upper) or RVF (lower).

It is also worth pointing out that a recent study revealed close association between microsaccades and covert visual attention, such that typical attention effects could be largely accounted for by microsaccades (Hafed, 2013). Therefore, although subjects were able to maintain gaze fixation at the central fixation cross (within 1°) in the present study, microsaccades may be functionally relevant to our findings, given the intimate link between microsaccades and exogenous attention (for a review, see Martinez-Conde et al., 2009). Future studies (e.g., record fine dynamics of microsaccades in a covert attention task) may be needed to investigate the rhythmic property of microsaccades and its possible relationship with the observed time-frequency profile of behavioral performances.

Finally, in the present study, the shortest SOA was designed to have more trials than other SOAs to enhance the cue resetting effect (Fiebelkorn et al., 2011). This is slightly different from other previous studies that had the same number of trials for all SOAs. Although using a somewhat different design, we argue that

the current findings cannot be accounted for by the difference of trial probability at the shortest SOA. First, a recent study with balanced numbers of trials for all SOAs also demonstrated rhythmic behavior (Landau and Fries, 2012). Second, although having more trials for the shortest SOA, we observed a similar attentional time course pattern as in classical findings of attentional effects, suggesting little influence of the present design on the classical attentional behavior. Therefore, having more trials for the shortest SOA may not be a key factor for whether a cue could phase reset perception and drive oscillations in behavior as demonstrated here. It awaits future studies to investigate if having imbalanced numbers of trials for different SOAs may lead to other behavioral effects.

Most importantly, our findings suggest a neural mechanism for attending to multiple spatial locations or items (i.e., when all of them are behaviorally relevant and therefore attended to simultaneously). Different from the biased competition model for selective attention (attending to one amid many) that is presumably mediated through neuronal γ-band synchronization by way of "communication-through-coherence" (Desimone and Duncan, 1995; Singer and Gray, 1995; Siegel et al., 2008), attending to multiple items would require unconfused and dissociated neural representation for each individual item. It has been postulated that θ rhythm constitutes the cycle of selection, by making and then breaking γ-band synchronization for selecting one item at a time within a cycle, thus enabling sampling for every relevant item and resulting in a rhythmic sampling of multiple items (Fries, 2009). In support, here we observed an alternation of α pulses between the two simultaneously attended spatial locations, mediated at an approximate θ rhythm, also consistent with pervious neurophysiological recordings revealing low-frequency oscillations associated with visual stimuli competition (Rollenhagen and Olson, 2005) and sensory selection (Schroeder and Lakatos, 2009). Although γ-band was not observed because of the limited sampling frequency here (50 Hz), the observed power-phase locking relationship between α and θ is conceptually commensurate with the proposed framework for attention to multiple items. Interestingly, similar synchrony-based dynamic formation, breaking, and reformation of distinct neuronal ensembles, to allow for population competition, have also been proposed and demonstrated in covert attention spotlight shifting (Buschman and Miller, 2009), working memory (Lisman and Idiart, 1995), consciousness (Doesburg et al., 2009), and task rule switching (Buschman et al., 2012). Moreover, our results are commensurate with the periodic sampling view in attention, positing that multiple items are processed in a serial manner, even when the attention is focused on a single target (VanRullen et al., 2007; Busch and VanRullen, 2010). In summary, combined with the known inhibitory nature of α power, our behavioral findings suggest that multiple items are explored in a temporally dissociated manner, such that each item or location is periodically sampled at a θ rhythm, by producing recurring inhibitory α pulses on nonrelevant neuronal ensembles.

References

Berens P (2009) CircStat: a Matlab toolbox for circular statistics. J Statist Software 31.

Bollimunta A, Chen Y, Schroeder CE, Ding M (2008) Neuronal mechanisms of cortical α oscillations in awake-behaving macaques. J Neurosci 28:9976–9988. CrossRef Medline

Bollimunta A, Mo J, Schroeder CE, Ding M (2011) Neuronal mechanisms and attentional modulation of corticothalamic α oscillations. J Neurosci 31:4935–4943. CrossRef Medline

Busch NA, VanRullen R (2010) Spontaneous EEG oscillations reveal periodic sampling of visual attention. Proc Natl Acad Sci U S A 107:16048–16053. CrossRef Medline

Buschman TJ, Miller EK (2009) Serial, covert shifts of attention during visual search are reflected by the frontal eye fields and correlated with population oscillations. Neuron 63:386–396. CrossRef Medline

Buschman TJ, Denovellis EL, Diogo C, Bullock D, Miller EK (2012) Synchronous oscillatory neural ensembles for rules in the prefrontal cortex. Neuron 76:838–846. CrossRef Medline

Buzsaki G (2006) Rhythms of the brain. New York: Oxford UP.

Canolty RT, Edwards E, Dalal SS, Soltani M, Nagarajan SS, Kirsch HE, Berger MS, Barbaro NM, Knight RT (2006) High γ power is phase-locked to θ oscillations in human neocortex. Science 313:1626–1628. CrossRef Medline

de Graaf TA, Gross J, Paterson G, Rusch T, Sack AT, Thut G (2013) α-band rhythms in visual task performance: phase-locking by rhythmic sensory stimulation. PLoS One 8:e60035. CrossRef Medline

Delorme A, Makeig S (2004) EEGLAB: an open source toolbox for analysis of single-trial EEG dynamics including independent component analysis. J Neurosci Methods 134:9–21. CrossRef Medline

Desimone R, Duncan J (1995) Neural mechanisms of selective visual attention. Annu Rev Neurosci 18:193–222. CrossRef Medline

Doesburg SM, Green JJ, McDonald JJ, Ward LM (2009) Rhythms of consciousness: binocular rivalry reveals large-scale oscillatory network dynamics mediating visual perception. PLoS One 4:e6142. CrossRef Medline

Fiebelkorn IC, Foxe JJ, Butler JS, Mercier MR, Snyder AC, Molholm S (2011) Ready, set, reset: stimulus-locked periodicity in behavioral performance demonstrates the consequences of cross-sensory phase reset. J Neurosci 31:9971–9981. CrossRef Medline

Fries P (2009) Neuronal γ-band synchronization as a fundamental process in cortical computation. Annu Rev Neurosci 32:209–224. CrossRef Medline

Giraud AL, Poeppel D (2012) Cortical oscillations and speech processing: emerging computational principles and operations. Nat Neurosci 15:511–517. CrossRef Medline

Hafed ZM (2013) Alteration of visual perception prior to microsaccades. Neuron 77:775–786. CrossRef Medline

Händel BF, Haarmeier T, Jensen O (2011) α oscillations correlate with the successful inhibition of unattended stimuli. J Cogn Neurosci 23:2494–2502. CrossRef Medline

Jensen O, Bonnefond M, VanRullen R (2012) An oscillatory mechanism for prioritizing salient unattended stimuli. Trends Cogn Sci 16:200–206. CrossRef Medline

Kayser C, Ince RA, Panzeri S (2012) Analysis of slow (θ) oscillations as a potential temporal reference frame for information coding in sensory cortices. PLoS Comput Biol 8:e1002717. CrossRef Medline

Klein RM (2000) Inhibition of return. Trends Cogn Sci 4:138–147. CrossRef Medline

Klimesch W (1999) EEG α and θ oscillations reflect cognitive and memory performance: a review and analysis. Brain Res Brain Res Rev 29:169–195. CrossRef Medline

Klimesch W, Sauseng P, Hanslmayr S (2007) EEG α oscillations: the inhibition-timing hypothesis. Brain Res Rev 53:63–88. CrossRef Medline

Landau AN, Fries P (2012) Attention samples stimuli rhythmically. Curr Biol 22:1000–1004. CrossRef Medline

Lisman JE, Idiart MA (1995) Storage of 7 ± 2 short-term memories in oscillatory subcycles. Science 267:1512–1515. CrossRef Medline

Luo H, Poeppel D (2007) Phase patterns of neuronal responses reliably discriminate speech in human auditory cortex. Neuron 54:1001–1010. CrossRef Medline

Luo H, Poeppel D (2012) Cortical oscillations in auditory perception and speech: evidence for two temporal windows in human auditory cortex. Front Psychol 3:170. CrossRef Medline

Luo H, Liu Z, Poeppel D (2010) Auditory cortex tracks both auditory and visual stimulus dynamics using low-frequency neuronal phase modulation. PLoS Biol 8:e1000445. CrossRef Medline

Luo H, Tian X, Song K, Zhou K, Poeppel D (2013) Neural response phase tracks how listeners learn new acoustic representations. Curr Biol 23:968–974. CrossRef Medline

Martinez-Conde S, Macknik SL, Troncoso XG, Hubel DH (2009) Microsaccades: a neurophysiological analysis. Trends Neurosci 32:463–475. CrossRef Medline

Mo J, Schroeder CE, Ding M (2011) Attentional modulation of α oscillations in macaque inferotemporal cortex. J Neurosci 31:878–882. CrossRef Medline

Ng BS, Schroeder T, Kayser C (2012) A precluding but not ensuring role of entrained low-frequency oscillations for auditory perception. J Neurosci 32:12268–12276. CrossRef Medline

Palva S, Palva JM (2007) New vistas for α-frequency band oscillations. Trends Neurosci 30:150–158. CrossRef Medline

Posner MI, Cohen Y (1984) Components of visual orienting. In: Attention and performance (Bouma XH, Bouwhuis DG, eds), pp 531–556. Hillsdale, NJ: Erlbaum.

Rohenkohl G, Nobre AC (2011) α oscillations related to anticipatory attention follow temporal expectations. J Neurosci 31:14076–14084. CrossRef Medline

Rollenhagen JE, Olson CR (2005) Low-frequency oscillations arising from competitive interactions between visual stimuli in macaque inferotemporal cortex. J Neurophysiol 94:3368–3387. CrossRef Medline

Romei V, Gross J, Thut G (2012) Sounds reset rhythms of visual cortex and corresponding human visual perception. Curr Biol 22:807–813. CrossRef Medline

Schroeder CE, Lakatos P (2009) Low-frequency neuronal oscillations as instruments of sensory selection. Trends Neurosci 32:9–18. CrossRef Medline

Siegel M, Donner TH, Oostenveld R, Fries P, Engel AK (2008) Neuronal synchronization along the dorsal visual pathway reflects the focus of spatial attention. Neuron 60:709–719. CrossRef Medline

Singer W, Gray CM (1995) Visual feature integration and the temporal correlation hypothesis. Annu Rev Neurosci 18:555–586. CrossRef Medline

Thut G, Nietzel A, Brandt SA, Pascual-Leone A (2006) α-band electroencephalographic activity over occipital cortex indexes visuospatial attention bias and predicts visual target detection. J Neurosci 26:9494–9502. CrossRef Medline

Thut G, Schyns PG, Gross J (2011) Entrainment of perceptually relevant brain oscillations by non-invasive rhythmic stimulation of the human brain. Front Psychol 2:170. CrossRef Medline

Thut G, Miniussi C, Gross J (2012) The functional importance of rhythmic activity in the brain. Curr Biol 22:R658–R663. CrossRef Medline

VanRullen R, Dubois J (2011) The psychophysics of brain rhythms. Front Psychol 2:203. CrossRef Medline

VanRullen R, Carlson T, Cavanagh P (2007) The blinking spotlight of attention. Proc Natl Acad Sci U S A 104:19204–19209. CrossRef Medline

Ward LM (2003) Synchronous neural oscillations and cognitive processes. Trends Cogn Sci 7:553–559. CrossRef Medline

Worden MS, Foxe JJ, Wang N, Simpson GV (2000) Anticipatory biasing of visuospatial attention indexed by retinotopically specific α-band electroencephalography increases over occipital cortex. J Neurosci 20:RC63. Medline